Presented at the Second Annual
Systems Simulation and Economic
Analysis Conference; San Diego, CA;
January 23 - 25, 1980.

BNL-27316

CONF-800101--17

OPTIMIZATION OF SOLAR ASSISTED HEAT PUMP SYSTEMS VIA A SIMPLE ANALYTIC APPROACH

John W. Andrews
Brookhaven National Laboratory
Building 701
Upton, New York
11973 USA

ABSTRACT

An analytic method for calculating the optimum operating temperature of the collector/storage subsystem in a solar assisted heat pump system is presented. A tradeoff exists between rising heat pump coefficient of performance and falling collector efficiency as this temperature is increased, resulting in an optimum temperature whose value increases with increasing efficiency of the auxiliary energy source. Electric resistance is shown to be a poor backup to such systems. A number of options for thermally coupling the system to the ground are analyzed and compared.

INTRODUCTION

Solar assisted heat pump (SAHP) systems have been studied extensively. Most of these studies [1-4] have simulated, on an hour-by-hour basis, several plausible system configurations involving solar collectors and heat pumps. All of the referenced studies assumed that electric resistance was the auxiliary heat source. Although much has been learned from these studies, it has been difficult to evaluate the sensitivity of their results to all of the assumptions that went into them. The need was seen for an approach which would be simple enough so that all of the assumptions could be stated concisely. Also, the question has been asked [5,6]: What is the optimum temperature at which solar energy should be collected and stored in SAHP systems? Such an optimum may be produced by the tradeoff between increasing heat pump coefficient of performance (COP) and decreasing collector efficiency with increasing temperature. This paper describes a method for answering the above question by means of closed-form algebraic solutions. Fundamental to the present approach is the assumption that, within acceptable limits of accuracy, the storage temperature of the solar system is a constant throughout each of the time periods (months in this paper) into which the simulation is divided. Of course, this will never be strictly true; however, in computer simulations of SAHP systems, the storage temperature during the period December through February, when most of the heating load occurs, remained most of the time within 10°C of the set minimum value. In any event, the outcome of the analysis will be an optimum storage temperature for each month; any excursions from this value will represent suboptimal operation.

COMPONENT MODELING

Collector performance is modeled via the usual Hottel-Whillier straight-line graph of efficiency vs. $(T-T_a)/I$. The collector inlet temperature is here assumed to equal the storage temperature T. Collector efficiency is given by

$$\eta = \eta_o \left(1 - \frac{1}{\chi_o} \cdot \frac{T-T_a}{I}\right) \qquad (1)$$

where T_a is the ambient temperature, I the insolation rate, and η_o and χ_o the vertical and horizontal intercepts of the efficiency curve.

The intensity of the insolation striking the collector during daylight hours is taken to be a random variable with a constant probability density for insolation values between 0 and I_{max}. That portion of received insolation falling with intensity greater than $(T-T_a)/\chi_o$ can be partially collected with efficiency increasing with increasing I. The lower-intensity insolation is lost completely. It can be shown that under these assumptions the total energy that can be collected at temperature T is given by

$$E_c = SA\eta_o \left(\frac{T_m - T}{T_m - T_a}\right)^2 \qquad (2)$$

where S is the received insolation on a unit area of collector, A is the collector area, and T_m is the maximum stagnation temperature $T_a + I_{max}\chi_o$.

The simple formula given in Eq. 2 is not intended to be exact, but in order for it to be useful it should provide results which are reasonably close to those given by more precise methods. I have therefore used Eq. 2 to calculate the solar fractions for the case given in the original f-Chart paper [7], assuming a collector operating temperature of 40°C, and I_{max} = 3410 kJ/m^2-hr. This comparison is shown in Columns 1-3 and 5-12 of Table 1. On a monthly basis Eq. 2 tends to give lower solar fractions than f-Chart at low collector areas and higher estimates at high collector areas. This trend is also seen in the yearly totals, with

*Work performed under the auspices of the U.S.Department of Energy, Systems Development Division, Office of Solar Applications.

DISCLAIMER

Table 1.

COMPARISON OF SOLAR FRACTIONS (f) OBTAINED USING EQ. 2 WITH THOSE OF f-CHART (f*). LOCATION: MADISON, WISCONSIN

Month	Heating & Hot Water Load (GJ)	Insolation on Tilted Collector (GJ/m^2)	Average Ambient Temperature (°C)	Far-Field Temperature (Ground Coupling) (°C)	$A = 20m^2$		$A = 40m^2$		$A = 80m^2$		$A = 120m^2$	
					f	f*	f	f*	f	f*	f	f*
Jan.	28.62	0.382	-8.1	3.3	0.08	0.11	0.16	0.23	0.32	0.42	0.48	0.56
Feb.	24.83	0.405	-6.0	0.8	0.13	0.15	0.26	0.30	0.51	0.53	0.77	0.69
Mar.	22.09	0.557	-0.2	0.1	0.18	0.25	0.36	0.47	0.72	0.76	1.00	0.91
Apr.	13.06	0.512	7.9	1.6	0.33	0.39	0.66	0.67	1.00	0.94	1.00	1.00
May	7.53	0.555	13.8	4.9	0.68	0.67	1.00	0.96	1.00	1.00	1.00	1.00
June	3.70	0.588	19.4	9.2	1.00	0.95	1.00	1.00	1.00	1.00	1.00	1.00
July	2.36	0.620	21.8	13.2	1.00	1.00	1.00	1.00	1.00	1.00	1.00	1.00
Aug.	2.63	0.600	20.9	15.9	1.00	1.00	1.00	1.00	1.00	1.00	1.00	1.00
Sept.	5.01	0.584	16.0	16.6	1.00	0.88	1.00	1.00	1.00	1.00	1.00	1.00
Oct.	10.51	0.522	10.5	15.0	0.43	0.47	0.86	0.77	1.00	1.00	1.00	1.00
Nov.	18.71	0.330	1.9	11.6	0.13	0.15	0.26	0.29	0.53	0.51	0.79	0.66
Dec.	26.02	0.357	-5.2	7.4	0.09	0.11	0.18	0.23	0.35	0.42	0.53	0.57
Year	165.07				0.25	0.28	0.41	0.44	0.62	0.65	0.78	0.76

Weather and load data (Columns 1-3 and f-Chart solar fractions)were taken from Ref. 7. Typical far-field temperatures (Column 4) were calculated for Madison using Ref. 12.

however closer agreement between the two at all collector areas. Because of its simplicity, Eq. 2 lends itself well to use in an analytical model of a more complicated system.

The coefficient of performance COP_h of the solar source heat pump is modeled as a constant fraction γ of Carnot [4]:

$$COP_h = \frac{\gamma T_c}{T_c - T} . \qquad (3)$$

The heat pump source temperature is assumed equal to the storage temperature T. In practice, a known curve of heat pump COP vs. source temperature can be fitted to this equation, with γ and T_c serving as parameters for the fit. This approach is taken here, with $\gamma = 0.596$ and $T_c = 345\ ^oK$ (based on data from Ref. 5). Because of the form of this equation, all temperatures must be expressed in absolute units in the work that follows.

In contrast to most computer simulations of SAHP systems to date, the auxiliary or backup energy source is not assumed at the outset to be electric resistance, with a COP of 1. Instead, the COP of the auxiliary (COP_x) is left as a parameter. We assume for now that the auxiliary COP is a constant independent of the extent to which it is used. Later, when ground coupling is considered, this assumption will have to be modified.

OPTIMUM OPERATING TEMPERATURE

It is now possible to consider the flows of energy through the system. The energy E_s delivered to the load by the solar source heat pump is equal to the sum of the collected solar energy plus the purchased energy needed to operate the heat pump, which is added to the heat delivered to the load:

$$E_s = \frac{COP_h}{COP_h - 1} E_c$$

$$= \frac{\gamma E_o (T_m - T)^2}{T_c (T - T_d)} \qquad (4)$$

where $E_o = SA\eta_o T_c^{\ 2}/(T_m - T_a)^2$, and $T_d = (1-\gamma)\ T_c$.

The purchased energy required is given by

$$E_{ps} = \frac{E_s}{COP_h}$$

$$= \frac{E_o (T_c - T)(T_m - T)^2}{T_c^2 (T - T_d)} . \qquad (5)$$

It is assumed here that the energy E_s delivered by the solar source heat pump does not exceed the load E_ℓ . In this case the auxiliary energy requirement is given by

$$E_x = E_\ell - E_s . \qquad (6)$$

The purchased energy required to operate the auxiliary is given by

$$E_{px} = \frac{E_x}{COP_x}$$

$$= \frac{E_\ell}{COP_x} - \frac{\gamma E_o (T_m - T)^2}{COP_x T_c (T - T_d)} . \qquad (7)$$

The total purchased energy $E_p = E_{ps} + E_{px}$ is to be minimized as a function of the solar system operating temperature by setting dE_p/dT equal to zero and solving for T. When this is done, the optimum operating temperature T_{op} is obtained:

$$T_{op} = \frac{T_r + 3T_d + \sqrt{(T_r - T_d)\ (T_r + 8T_m - 9T_d)}}{4} \quad (8)$$

where $T_r = (1 - \gamma/COP_x)T_c$.

One should remember that this result depends upon the assumption that the energy E_s delivered by the solar source heat pump does not exceed the load E_ℓ . This requirement defines a domain of reasonable storage temperatures, the lower limit of which is the temperature T_{ox} for which enough solar energy is collected that no auxiliary is needed. Below this temperature, the theory presented above no longer corresponds to reality, since it would require a negative contribution from the auxiliary. But there can be no point in going below this temperature in practice, since heat pump performance becomes poorer and there is no compensating reduction in auxiliary usage. By setting E_s equal to E_ℓ and solving for T, the no-auxiliary storage temperature T_{ox} is obtained:

$$T_{ox} = T_m + \frac{E_\ell T_c - \sqrt{4\gamma E_o E_\ell T_c (T_m - T_d) + E_\ell^2 T_c^2}}{2\gamma E_o} \quad . (9)$$

If $T_{op} > T_{ox}$, then the assumptions used in deriving T_{op} are valid and T_{op} is the optimum storage temperature. If $T_{op} < T_{ox}$, then T_{op} is unphysical and T_{ox} is the optimum. In any case, then, the optimum storage temperature T_o is given by

$$T_o = \max \left\{ T_{op},\ T_{ox} \right\} \quad (10)$$

A number of conclusions can be drawn from this analysis. First, if electric resistance auxiliary is used ($COP_x = 1$), then $T_r = T_d$ and

$$\frac{dE_p}{dT} = \frac{2E_o(T_m - T)}{T_c^2} \quad . \quad (11)$$

The right side of Eq. 11 is positive for all $T < T_m$; therefore the purchased energy required decreases monotonically with decreasing T and there can be no optimum $T_{op} > T_{ox}$. In this case T_{ox} is always the optimum temperature, which means that the system should be operated at a temperature low enough to make resistance backup unnecessary. For low collector areas T_{ox} can be well below ambient, possibly resulting in system performance poorer than that of an air-to-air heat pump. But it does lead to the conclusion that resistance heat is a poor backup to such a system, since if it needs to be used it implies suboptimal system operation.

If a backup with a COP greater than one is used, then optimum operating temperatures can be obtained which require the use of some backup. Such an auxiliary could be provided, for example, by a separate, freezable tank of water or other phase-change material (a mini-ACES system), or, on a primary energy basis, by a fossil-fueled burner. If such an auxiliary is used, one can obtain the optimum storage temperature for the SAHP system for each month, and the amount of purchased energy required to operate the system. One can also calculate the energy required to meet the entire load with the auxiliary only, without the SAHP. For some types of auxiliary (e.g. the ice-maker) this latter strategy would involve added capital and operating costs, whereas for others (e.g. the fuel-fired burner) there would be no additional capital costs. The difference between these two numbers is the energy saved by the SAHP system. These energy savings are presented in Fig. 1, for the weather and load data of Table 1, as functions of collector area, for systems having auxiliaries with COP's of 2, 2.4, and 3. Collectors having vertical intercepts of 0.7 and horizontal intercepts of 0.02, 0.03, and 0.04 °C-m^2-hr/kJ are used. As the efficiency of the auxiliary increases, the energy which can be saved by the SAHP system decreases relative to use of the auxiliary only. There are two reasons for this. First, with a more efficient auxiliary there is simply less room for conservation since the auxiliary is now by itself relatively energy efficient. Second, the SAHP, in order to compete with the auxiliary, must operate at higher source temperatures in order to provide COP's that are attractive relative to the auxiliary. This can be seen by examining in Fig. 1 the January (lowest) optimum storage temperatures for each case. Operating at higher source and collection temperatures, the SAHP system will now collect and use less solar energy than before. In evaluating these results, it is necessary to keep in mind the assumption that was made, that the auxiliary COP was independent of the extent to which it is used. A more efficient auxiliary which uses electricity as the source of purchased energy must use a heat pump in connection with an alternate source of low-grade heat, as from

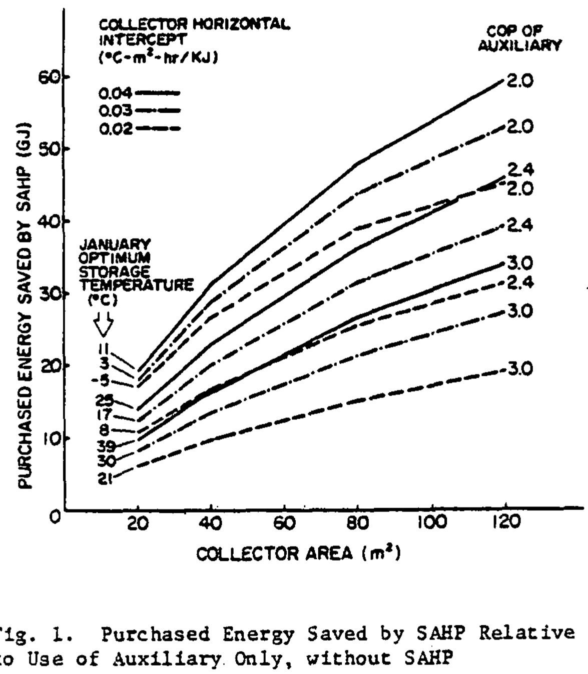

Fig. 1. Purchased Energy Saved by SAHP Relative to Use of Auxiliary Only, without SAHP

the latent heat of fusion of ice or from the ground. Such auxiliaries will in general not satisfy the above assumption of constant COP as a function of utilization, but will perform better when used less or, alternatively, will require greater initial capital cost to provide the same performance at higher levels of utilization. One possible alternate heat source, the ground, is now examined in greater detail.

GROUND COUPLING

The use of the ground as a source of low-grade heat as input to a heat pump for space and water heating is under intensive investigation in a number of countries [8-10]. A number of options for combining the use of ground-source and solar-source energy have been indentified. These are:

1. Use of the ground as a long-term solar storage medium, to allow excess solar heat collected in the summer and fall to be partially recovered in the winter months.

2-4. Storage of solar heat in a separate tank, with ground heat processed to the load via the heat pump when solar heat is unavilable. At least three substrategies exist:

2. Solar heat delivered to the load directly when the tank temperature is above a set minimum (here taken to be 40°C), and processed through the heat pump when the tank temperature is less than this.

3. Solar heat delivered to the load directly only. Ground-coupled auxiliary is used when the tank temperature drops to 40°C.

4. Solar heat used to preheat the return air from the load, with use of the ground-source heat pump to raise the air temperature to the value required for comfort [3]. In this strategy the tank temperature can drop below 40°C, but must remain above that of the heated space (20°C).

5. Use of passive solar design concepts, with the ground-coupled heat pump providing hot water and auxiliary space heating.

Although the present study concentrates on heating, it should be remembered that in each of these concepts the heat pump can also provide sensible cooling and/or dehumidification, where required. The following analysis begins with option 2, and is extended to options 3 and 4. Treatment of options 1 and 5 remains for future work. Other means of combining solar with ground energy are possible, such as the burning of wood backed up by the ground-source heat pump or the use of photovoltaics to drive the ground-source heat pump. These are not considered here.

System Optimization for Option 2

In order to treat the case where ground-source heat is used as a backup to a solar-source heat pump, it is assumed that the ability of the ground to deliver heat is proportional to the difference between the temperature T_x at which heat is extracted and the temperature T_f of undisturbed ground at the same depth at the same time of the year, or far-field temperature:

$$E_g = (T_f - T_x)\, b \tag{12}$$

The constant b is a product of the inherent heat transfer capability of the ground coupling device, in kJ/hr-°C-m for linear pipes or kJ/hr-°C-m^2 for tanks or planar devices; the size of the device in linear or square meters; and the number of hours in the time period, e.g. 720 hr/month. The COP of the heat pump using ground-source energy is assumed to follow the same function of source temperature as when using solar-source energy:

$$COP_x \equiv \frac{E_x}{E_{px}} = \frac{\gamma T_c}{T_c - T_x} \tag{13}$$

Two energy balance equations can be written, the one on the ground-source heat pump given by

$$E_x = E_g + E_{px} \tag{14}$$

and the one on the load given by Eq. 6 as before.

Solving these equations for E_{px} (eliminating E_x, E_g, and T_x) one obtains

$$E_{px} = \frac{(E_\ell - E_s)\,(E_\ell - E_s + bT_c - bT_f)}{b\gamma T_c + E_\ell - E_s} \tag{15}$$

where E_s is given as a function of T by Eq. 4. E_{px} is then added to E_{ps} to obtain E_p, the function to be minimized. The functional relationship between E_p and T is now complicated enough that attempting to find the minimum in the usual way results in an intractable fourth-degree equation. Instead, the minimum was found for each case by means of a computer. The COP vs. T relationship used (including parasitic power requirements) is shown in Fig. 2, which assumes processing of solar heat through the heat pump below 40°C [5] and direct heating above [11]. For the latter region of temperature, the above equations were modified to take into account the linear relationship of direct-heating COP to temperature T.

The relationship of solar collector area to ground-coupled field heat-transfer capacity, for systems optimized as to storage temperature on a monthly basis, is shown by the solid curves in Figs. 3-5 for collectors having horizontal intercepts χ_o equal to 0.02, 0.03, and 0.04 °C-m^2-hr/kJ, respectively. The weather and load data of Table 1 were used. Representative far-field temperatures were calculated at 1.5m depth at the Madison location [12]. Each curve is plotted for a constant fraction F of nonpurchased (solar and/or ground) energy. The numbers along the curve are the optimum operating temperatures for solar storage, in January, at that point on the curve.

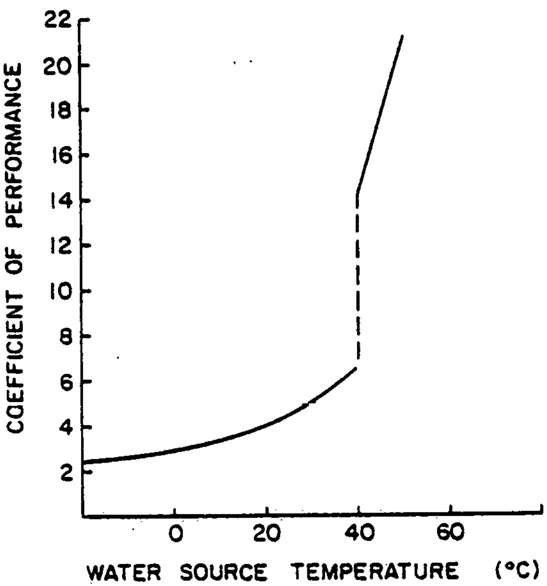

Fig. 2. System COP vs. Water Source Temperature: T<40°C, Heat Pump; T>40°C, Direct Heating.

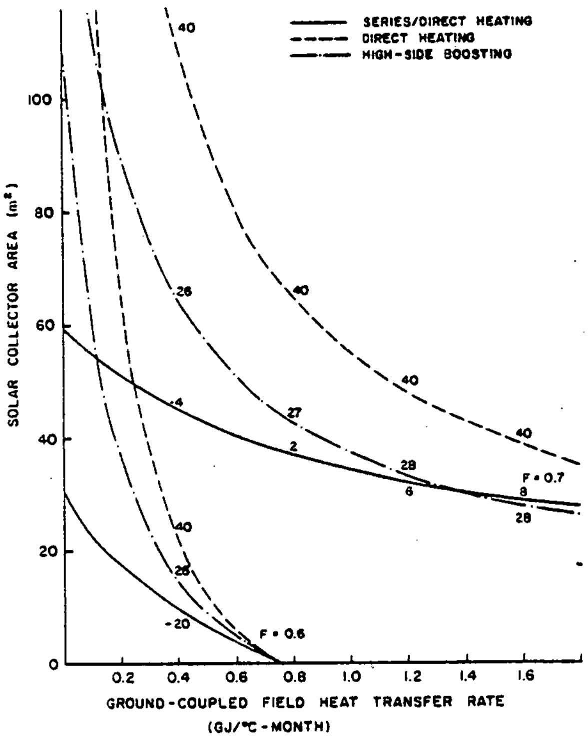

Fig. 3. Solar Collector Areas and Ground-Coupled Field Sizes Needed to Provide a Fraction F of Non-Purchased Energy. Horizontal Intercept X_o of Collector Efficiency Curve = 0.02°C-m^2-hr/kJ. Numbers on Lines Are Optimum Source Temperatures in January.

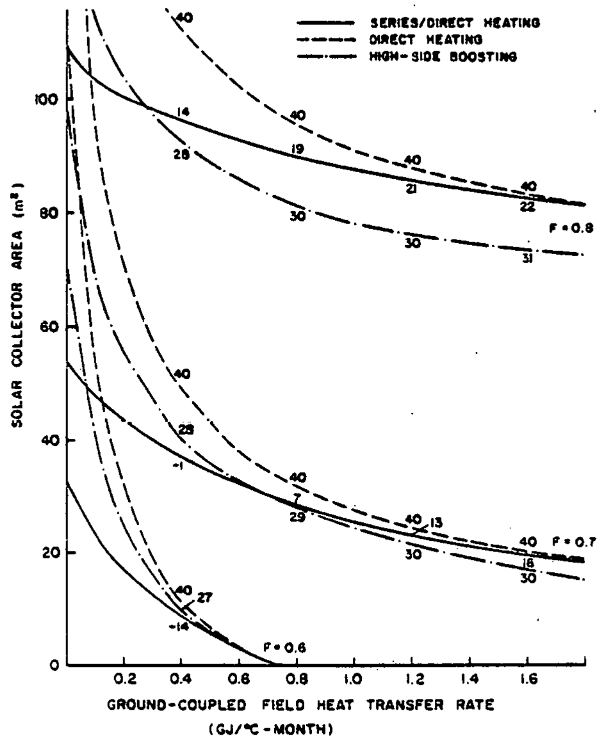

Fig. 4. Solar Collector Areas and Ground-Coupled Field Sizes Needed to Provide a Fraction F of Non-purchased Energy, X_o = 0.03°C-m^2-hr/kJ.

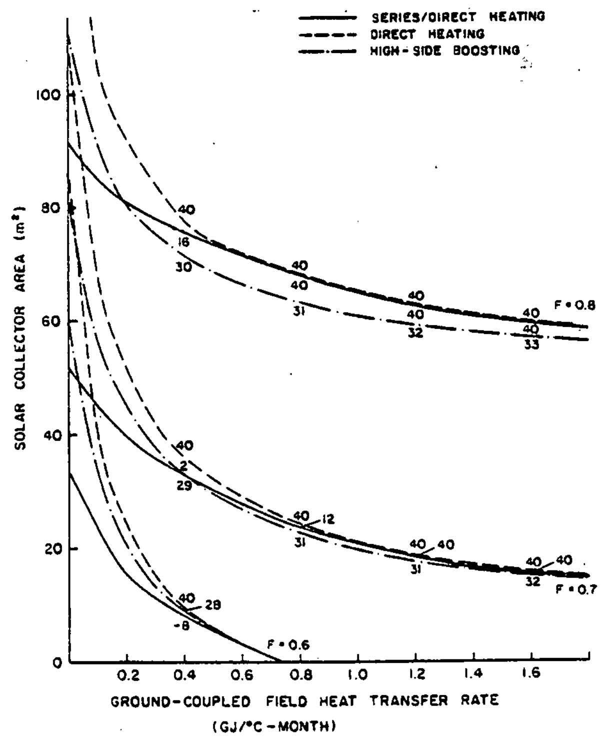

Fig. 5. Solar Collector Areas and Ground-Coupled Field Sizes Needed to Provide a Fraction F of Non-Purchased Energy, X_o = 0.04°C-m^2-hr/kJ.

Economic Optimum

The tradeoff between solar collector area and ground coupling can be represented by curves of constant cost, which are straight lines whose negative slope is equal to the ratio of unit cost of ground coupling to that of collector area. From a family of such lines of equal slope, select the one which is tangent to the curve of constant system performance. The economic optimum, for a preselected fraction of nonpurchased energy, for systems having both solar collectors and ground coupling, is the point of tangency. Bose [9a] has quoted an installed cost of \$2 to \$3/ft (\$6.50 to \$10/m) for a buried-pipe system which provides sustainable heat rates in excess of 2 Btu/hr-°F-ft pipe (12.5 kJ/hr-°C-m pipe). If collectors are assumed to cost \$100/m^2 or more installed, optimum ground-coupled field capacities of approximately 1.0 GJ/°C-month or more are obtained. This is important to the discussion which follows.

Options 3 and 4

The analysis was extended to include option 3 by restricting the computer search of solar source temperatures to a domain above 40°C. Curves of constant system performance for systems optimized under these conditions are shown by the dashed lines in Figs. 3-5. Since the set of possible operating conditions under option 3 is a proper subset of those available to option 2, the option 3 curves will always lie at or above those of option 2. For option 3 the January optimum operating temperature was always 40°C, the minimum available.

An approximate treatment of option 4 was made by allowing the search for the optimum temperature under the direct heating mode to extend below 40°C, with a COP as a function of temperature which follows the same straight line as above 40°C, intercepting the horizontal axis at 20°C (slope 0.7/°C). The results of this optimization procedure are shown by the dash-dot lines of Figs. 3-5.

Results for Ground Coupling

If we focus our attention towards the right sides of Figs. 3-5, where in each case the economic optimum probably lies, the following results can be noted. For the two better collectors (Figs. 4 and 5), options 2 and 3 gave results which were not very different. Since option 3 is operationally simpler than option 2, it is to be preferred in these cases. Option 4 gives somewhat better results than the others, but the difference is not great except for F=0.08, χ_o = 0.03 (Fig. 4). For the collector having the lowest horizontal intercept (Fig. 3), option 2 requires significantly less collector area than option 3. In this case, option 4 is about equivalent in performance to option 2. Option 4, while more complex from a controls standpoint than option 3, is about as simple as option 3 as far as hardware is concerned, and is therefore probably to be preferred over option 2 in this case.

CONCLUSIONS

The following conclusions are drawn: 1) Electric resistance is a poor backup to a SAHP system. 2) As the COP of the auxiliary increases, the optimum storage temperature of the SAHP system increases, assuming that the auxiliary COP is independent of the extent to which it is used. 3) When ground coupling is used as a backup to a SAHP system, and solar energy is collected in a separate tank, it does not appear advantageous to process solar-derived heat through the heat pump. This conclusion does not apply to the case where solar energy is stored in the ground.

REFERENCES

1. T.L. Freeman, J.W. Mitchell, and T.E. Audit, Performance of combined solar heat pump systems, Solar Energy 22, 125-135 (1979).
2. P.J. Hughes and J.H. Morehouse, Comparison of solar heat pump systems to conventional methods for residential heating, cooling, and water heating, Science Applications Inc., McLean Virginia, Report 80-906-WA (1979).
3. B.C. Hwang and W.F. Bessler, Economics of solar assisted heat pump systems for residential use, International Solar Energy Society International Congress, Atlanta (1979).
4. W. Kahan and R.C. Estes, Optimization and comparison strategies for solar energy systems, Am. Soc. Mech. Eng. Pub. 79-WA/SOL-26 (1979).
5. E.A. Kush, Performance of heat pumps at elevated evaporating temperatures - with application to solar input, ASME Pub. 79-WA/SOL-19 (1979).
6. P. Vercaemert et al., A simplified procedure for performance of solar systems with heat pumps, ASME Pub. 79-WA/SOL-23 (1979).
7. S.A. Klein, W.A. Beckman, and J.A. Duffie, A design procedure for solar heating systems, Solar Energy 18, 123-4 (1975).
8. P. Metz, Experimental results from the solar ground coupling research facility at Brookhaven National Laboratory, International Solar Energy Society International Congress, Atlanta (1979).
9. J.E. Bose, Design and field testing of solar assisted earth coils, Annual Report, U.S. Dept. of Energy Contract EM-78-S-01-4257, Oklahoma State University (1979); a, p. 18.
10. Many papers on ground coupling are collected in the Proceedings of the Nordic Symposium on Earth Heat Pump Systems, Chalmers University of Technology, Göteborg, Sweden, October 1979.
11. W. Dollars et al., Development of marketable solar assisted heat pumps - residential design review, Lennox Industries Inc., Carrolton Texas, p. 1-3 (1978). Report prepared under U.S. Dept. of Energy contract EG-78-C-03-1720.
12. K. Labs, Underground building climate, Solar Age 4, No. 10, pp. 44-50 (October 1979).